CONFINED TURBULENT FLUID-PARTICLE FLOW MODELING USING MULTIPLE-REALIZATION PARTICLE TRAJECTORY SCHEMES

A. A. Adeniji - Fashola

NRC Research Associate
NASA - Marshall Space Flight Center
Huntsville, AL. 35812

ABSTRACT

A multiple-realization particle trajectory scheme has been developed and applied to the numerical prediction of confined turbulent fluid-particle flows. The example flows investigated include the vertical pipe upflow experimental data of Tsuji et al. and the experimental data of Leavitt for a coaxial jet flow, comprising a particle-laden central jet and a clean annular jet, into a large recirculation chamber. The results obtained from the numerical scheme agree well with the experimental data lending confidence to the modeling approach. The multiple-realization particle trajectory turbulent flow modeling scheme is believed to be a more elegant and accurate approach to the extension of single-particle hydrodynamics to dilute multi-particle systems than the more commonly employed two-fluid modeling approach. It is also better able to incorporate additional force terms such as lift, virtual mass and Bassett history terms directly into the particle equation of motion as appropriate. This makes it a suitable candidate for particle migration studies and an extension to situations involving liquid particulate phases with possible propulsion applications, such as in spray combustion, follows naturally.

INTRODUCTION

Turbulent fluid-particle flows are encountered in numerous technological applications such as fluidized-bed combustors and pulverized coal gasifiers and combustors as well as in atmospheric studies involving the dispersion of pollutants. The modeling of such turbulent flows involving the presence of a dispersed phase made up of small, light particles further complicates the already complex phenomena encountered in single phase turbulent flows. However, the need to optimize the design process in technological applications involving turbulent fluid-particle flows or enhance the prediction accuracy of atmospheric dispersion models makes it impossible to avoid the quest for a deeper understanding of the fundamental problems. Besides, the various interacting complex phenomena encountered in the modeling of this class of flows offer a very rich source of challenges to the fluid flow researcher.

The propulsion systems for space transportation vehicles, in particular the liquid-fueled variety, will benefit directly from an improvement in the modeling of turbulent fluid-particle flows. This is because such an improvement will translate to a better understanding of the mixing and combustion phenomena in spray combustion processes. Turbulent fluid-particle flows involving solid particles are simpler to model than fluid-droplet or fluid-bubble flows due to the added degrees of freedom in the latter associated with the deformation of the discrete entities of such a dispersed fluid phase. A study of turbulent fluid-solid particle flows is thus useful in eliminating the effects of the breakup or coalescence of droplets and bubbles from other particle-turbulence interactions encountered in such flows.

The two common approaches adopted in the literature for the modeling of two-phase flows are the homogeneous and the separated models. The former is applicable to situations in which the mean slip between the phases is small and the design parameters of interest are of the bulk variety such as the pressure drop or mass fluxes. In situations where more detailed information about intra- or inter-phase behavior is of interest, or where there is substantial segregation of the phases, the separated two-phase models are invariably preferred. For such flows, another major decision has to be made with regard to the scheme for the description of the dispersed phase - whether to adopt an Eulerian or a Lagrangian approach. Important considerations necessary for deciding which approach to adopt include the concentration of the dispersed phase which influences the mean separation distance between particles. The relative magnitudes of this length scale as well as the particle size and the microscale of the underlying turbulence in the continuous phase help to determine whether the dispersed phase can be treated as a continuum and thus described using the Eulerian approach or whether a Lagrangian description of the dispersed phase will be more appropriate.

In the following, we present a discussion of turbulent fluid-particle flow

modeling in which the continuous phase is described using the continuum Eulerian approach while a Lagrangian description is adopted for the dispersed phase. We shall restrict ourselves to confined flows and thus include a discussion of the treatment of solid boundaries using the Eulerian - Lagrangian scheme.

2. PARTICLE TRAJECTORY SCHEMES

In the Eulerian - Lagrangian modeling of two-phase flows, the continuous fluid phase is described using the standard single phase continuum equations. However, the dispersed phase is modeled by computing for individual particles the trajectories and temperature histories where appropriate. The dispersed phase velocity and temperature fields are subsequently obtained from information obtained from the realization of a sufficiently large ensemble of particle trajectories.

The use of a particle trajectory scheme in the modeling of turbulent fluid-particle flows represents only a subset in the field of computer simulation using particles as discussed by Hockney and Eastwood [1981]. Other important applications particle schemes discussed by Hockney and Eastwood include the modeling of covalent and ionic liquids, stellar and galaxy clusters, plasma and semiconductor devices.

In fluid dynamic applications, the Particle-In-Cell (PIC) method of Harlow [1964] and, later, the Particle-Source-In Cell (PSI-Cell) method of Crowe et al. [1977] have received considerable attention. In the present investigation, the PSI-Cell method has been adopted as the basis for the Eulerian - Lagrangian model developed.

The usual starting point for the development of fluid-particle flow theory is the consideration of the motion of a single particle in an infinite fluid. The nature of such a single-particle flow has been investigated by numerous researchers including Bassett [1888], Boussinesq [1903], Oseen [1927], Tchen [1947], Corrsin and Lumley [1956] ,Hjelmfelt and Mockros [1966] and Maxey and Riley [1983] and is relatively well understood for flows both within and outside of the Stokes flow regime. In the Eulerian treatment of the dispersed phase, the single particle flow theory is adopted directly to describe a multi-particle system and the validity of such a step is assumed. However, in the Lagrangian particle tracking approach, the focus remains on single particle hydrodynamics for obtaining an ensemble of statistical realizations, in this case the particle trajectories, which are then analyzed using the well established mathematical theory of statistics to extract the required phase information.

In the presence of turbulence, particle trajectories are not deterministic due to an imposition over the mean velocity of a rapidly fluctuating random velocity component. This additional velocity component due to turbulence enhances the

dispersion of the particles, in aggregate, while the presence of the particles in the continuous phase, even in relatively small concentrations [Al-Taweel and Landau 1977], does modify the underlying turbulence appreciably. This 'two-way coupling' between the turbulence and the particulate phase exercises considerable influence over the evolution of such flows. These important effects will be considered later.

3. GOVERNING EQUATIONS

The field equations for the continuous phase in the Eulerian - Lagrangian scheme are the same as those for single phase flows except for the addition of an extra 'source' term which accounts for the influence of the particulate phase on the continuous phase. The equations are written in a generalized form as

$$\frac{\partial}{\partial x_i}(\rho u_i \phi) = \frac{\partial}{\partial x_i}\left(\Gamma_{eff}\frac{\partial \phi}{\partial x_i}\right) + S + S_p \qquad (3.1)$$

where u_i are the instantaneous velocity components, Γ_{eff} the effective exchange coefficients, S the usual single-phase source terms, S_p the source terms due to the particulate phase and ϕ any of the field variables such as velocity component, temperature for flows involving energy exchange, turbulence kinetic energy or its dissipation rate.

The simplified form of the particle trajectory equation in which only the hydrodynamic drag term between the phases is retained [Adeniji-Fashola and Chen, 1987] is

$$\frac{dv_i}{dt} = \frac{(u_i - v_i)}{\tau_*} \qquad (3.2)$$

where, in general, the fluid and particle velocities, u_i and v_i respectively are made up of a mean and a fluctuating component and τ_* is a particle response time defined in terms of the particle relaxation time t_* which is valid for particle motion within the Stokes regime. Thus we have

$$u_i = U_i + u_i' \qquad (3.3)$$

$$v_i = V_i + v_i' \qquad (3.4)$$

$$\tau_* = t_*/f \tag{3.5}$$

where

$$t_* = \frac{\rho_s d_p^2}{18\,\mu} \tag{3.6}$$

and

$$f = \frac{C_D Re_p}{24} = \begin{cases} 1 & \text{FOR } Re_p = \dfrac{|U_i - V_i| dp}{v} \leq 1 \\ 1 + 0.15\, Re_p^{0.687} & \text{FOR } Re_p > 1 \end{cases} \tag{3.7}$$

An expression similar to equation (3.2) for the particle temperature history written for a particle thermal equilibration time t_{TH} can also be written for flows involving energy transfer [Chen and Adeniji-Fashola, 1987].

4. PARTICLE-TURBULENCE INTERACTION

A very important aspect of the modeling of turbulent fluid-particle flows is the particle-turbulence interaction problem. Turbulence kinetic energy extracted from the mean flow kinetic energy of the continuous phase is partly dissipated by the smallest eddies and partly imparted to the particles thus enhancing the dispersion of the particulate phase. This 'two-way coupling' referred to earlier - modulation of the kinetic energy of turbulence by the particles and enhanced dispersion of the particles by the turbulence will now be discussed in a little more detail. It is pertinent to point out at this point that the turbulent dispersion phenomenon is primarily responsible for the considerable enhancement in mixing observed for turbulent flows when compared with laminar flows.

TURBULENT DISPERSION

The turbulent dispersion phenomenon is very closely related to the interaction between individual particles and turbulent eddies. A particle normally interacts with a series of eddies as it moves through the fluid. The particle trajectory scheme attempts to simulate this interaction by tracking each repre-

sentative computational particle through a succession of turbulent eddies contained within the domain of interest. Figure 1 is a schematic illustration of this interaction between particle and eddies and in relation to the computational cells. As discussed by Gosman and Ioannides [1981], a particle interacts with a given eddy for a period of time which is the minimum between an estimated particle transit time within the eddy, t_{tr} and an eddy lifetime, t_e. The particle transit time is obtained as the solution of the linearized equation of motion of the particle while the Lagrangian time scale of the turbulent eddy is obtained from length and velocity scales of the turbulence which are extracted from a k- turbulence model. Thus,

$$t_{int} = \text{Min}\,[t_e, t_{tr}] \tag{4.1}$$

where

$$t_{tr} = -t_* \ln [1.0 - l_e/t_* |u_i - v_i|] \tag{4.2}$$

and

$$t_e = l_e/(2k/3)^{1/2} \tag{4.3}$$

The eddy length macroscale, l_e is defined in terms of the kinetic energy of the turbulence, k and its dissipation rate, ε as

$$l_e = C_\mu^{3/4} k^{3/2}/\varepsilon \tag{4.4}$$

In a stochastic formulation of the particle trajectory scheme which is the case in the present study, the fluctuating component of the fluid velocity, u', is obtained from a Gaussian distribution of values having a zero mean and a standard deviation, σ_{ii} given by

$$\sigma_{ii} = (2k/3)^{1/2} \tag{4.5}$$

The Gaussian distribution is, however, not expected to be appropriate, in general, for describing non-homogeneous, non-turbulent flows.

TURBULENCE MODULATION

The presence of particles, even in very small concentrations, has the effect of modulating the turbulence intensity, the direction of modulation being influenced by the mean particle size and the level of modulation by the particle loading. This turbulence modulation effect was observed experimentally by Moderrass et al. [1984] and Tsuji et al. [1984] and attempts to mathematically characterize the phenomenon include those of Al-Taweel and Landau [1977] and Chen and Wood [1985]. The interphase interaction force terms between particles and the continuous phase are reflected as extra dissipation terms in the modeled equations for k and ε when the former are included in the derivation of the field equations for the latter. The earlier attempts to implement these turbulence modulation models have been mostly within a two-fluid formulation in which the two phases are described as two interpenetrating continua viewed from an Eulerian framework. Equations (4.6) and (4.7) from Chen and Wood [1986] show the extra dissipation terms due to the turbulence modulation effect of the particles for such a two-fluid formulation:

$$\frac{\partial}{\partial x_j}(U_j k) = \frac{\partial}{\partial x_j}\left(\frac{\nu_t}{\delta_K}\frac{\partial k}{\partial x_j}\right) + P_K - \varepsilon - \underbrace{\frac{\overline{\rho_p u_i}}{\rho t_*}(1+0.15Re_p^{0.687})(U_i-V_i)}_{(TH1)} - \underbrace{\frac{2k}{t_*}\frac{\overline{\rho}_p}{\rho}[1-\exp(-0.5\, t_*\varepsilon/k)]}_{(TH2)} \tag{4.6}$$

$$\frac{\partial}{\partial x_j}(U_j \varepsilon) = \frac{\partial}{\partial x_j}\left(\frac{\nu_t}{\delta_\varepsilon}\frac{\partial \varepsilon}{\partial x_j}\right) + \frac{\varepsilon}{k}(C_1 P_K - C_2 \varepsilon) - \underbrace{2\frac{\overline{\rho}_p}{\rho}\frac{\varepsilon}{t_*}}_{(TH3)} \tag{4.7}$$

The term TH1 in equation (4.6) is the turbulence modulation term due to the mean slip while the terms TH2 and TH3 are due to the particle slip velocity at the fluctuating level. The model is valid for the situation

$$t_e > t_* > t_K , \qquad \text{where} \qquad t_K = (\nu/\varepsilon)^{1/2} \tag{4.8}$$

is the Kolmogorov time scale. The model described above has been incorporated into the particle trajectory scheme of the present study.

5. NUMERICAL SCHEME

The set of governing differential equations describing the evolution of confined turbulent fluid particle flows cannot, in general, be solved analytically thus requiring the adoption of a numerical procedure. For the continuous phase, the governing Eulerian equation set is solved using the SIMPLE algorithm of Patankar and Spalding [1972] and Patankar [1980]. The overall scheme adopted for the solution of the governing equations is similar to that suggested by Crowe et al. [1977] and illustrated in Figure 2. An alternative scheme more suited to time-dependent flows was later presented by Dukowicz [1980] and further developed by Cloutman et al. [1982] and Amsden et al. [1985].

First, the "clean" fluid flow field is obtained by solving the continuous phase governing equations. This is done using a staggered grid distribution in which velocity cells are centered about the edges of the scalar cells. Next, particle trajectories are computed for a predetermined number of representative particles such that a statistically stationary solution is obtained for the overall particle flow field. The particle trajectories, and temperature history where appropriate, are obtained by solving for the particle the non-linear ordinary differential equations of motion and the energy equation subject to the currently existing continuous fluid flow and temperature fields. A fourth order Runge-Kutta algorithm is used for this purpose. During the calculation of a particle's trajectory and temperature history, the sources of momentum, energy, kinetic energy of turbulence and its dissipation rate, all due to the particle motion, are accumulated for each computational cell traversed. The form of the source terms have already been presented elsewhere [Adeniji-Fashola and Chen, 1987] and so will not be repeated here. These source terms are then used in the next global iteration on the continuous phase field equations until convergence is attained. It was found that source term relaxation was required to achieve stability of the global iteration scheme for some of the example flow problems studied.

PARTICLE SOURCE FIELD CONTINUITY

A necessary condition to obtain a globally converged solution is to ensure the continuity of the source fields as was also pointed out by Durst et al. [1984]. In order to ensure compliance with this important requirement, it is necessary to ensure the computation of source terms for each cell traversed by each computational particle through a judicious choice of the particle integration time step as well as have particles start from as many locations as is

practicable within the relevant portion of the inlet plane. In the present study, particles are uniformly distributed in physical space at the appropriate portion of the inlet plane of the computational domain in contrast to the scheme of Durst et al. [1984], in which particles are introduced only at grid nodes. The smooth profiles they obtained are very likely to be a consequence of the deterministic nature of the particle trajectories used in their study.

INTEGRATION TIME STEP

The choice of appropriate time steps for the integration of the particle equations of motion is very vital to obtaining a globally converged solution and smooth averaged particle flow fields. For the complex confined turbulent fluid-particle flow problems in general, some of the relevant time scales include the Lagrangian or macro time scale (eddy lifetime) of the turbulence, t_e; the Kolmogorov or the micro (dissipation) time scale of the turbulence, t_K; the particle relaxation time, t_*; the particle residence time within a computational cell or the whole computational domain t_R. Also relevant to the stochastic determination of the particle turbulent intensity are the particle transit time within an eddy, t_{te} and the particle eddy interaction time, t_{int}. The integration time step is selected to ensure adequate resolution with regard to the trajectory and temperature evolution while ensuring computational efficiency by avoiding unnecessarily small time steps.

In the present study, a variable integration time step scheme was devised. An upper bound on the time step through any computational cell was imposed based on an estimated particle residence time for that cell and with the particle being constrained to undergo about four integration steps within the cell. Without this restriction, the possibility of a particle overshooting one or more cells, possibly due to a sudden reduction in cell dimensions in a non-uniform grid domain, exists. Such a situation will result in a failure to compute the relevant source term contributions for a cell that was actually traversed by the particle. The consequence will be a lack of smoothness in the particle source distribution and, possibly, divergence of the global iterations.

Also, for the reason of ensuring a smooth evolution of the particle trajectory and temperature history, a further restriction on the integration time step, $\Delta t < t_*$, is made. The particle-eddy interaction time is determined and controlled independently of the integration time step.

PARTICLE AVERAGED PARAMETERS FROM PARTICLE TRAJECTORY STATISTICS

One of the problems associated with the use of the Lagrangian particle trajectory approach, highlighted by Smoot and Smith [1985], is the difficulty of extracting smooth mean particle flow and temperature fields from the statistics of trajectories and temperature histories obtained for representative computational particles. In the present study, the fluid properties utilized in the particle trajectory and temperature history calculations are the linearly interpolated values in which the four nearest neighbors regarding the particle's current location are used, resulting in second order accuracy [Sirignano, 1983]. The details of the extraction of particle mean flow and temperature fields information from the particle trajectory and temperature history statistics are available in Adeniji-Fashola et al. [1988].

BOUNDARY CONDITIONS

The definition of a fluid flow problem becomes unique through the specification of the boundary conditions after the governing differential equations are outlined and an appropriate closure of these equations is effected. The example flow problems investigated in the present study include vertical pipe upflow and horizontal recirculation chamber flow. However, rather than define the boundary conditions specific to each flow problem separately, the more efficient approach of defining generic boundary condition types is adopted. It then becomes a straightforward exercise to construct the boundary conditions for these and other specific flow situations of interest.

Inlet Plane:

The specification of the inlet plane boundary conditions for fluid flow problems is very important, as was discussed by Sturgess et al. [1983] and Westphal and Johnston [1984], since this influences significantly the subsequent evolution of the flow, especially in the case of parabolic flows for which the inlet plane conditions constitute the initial conditions for the solution of the governing differential equations.

In order to correctly simulate a given fluid flow experiment numerically, the ideal specifications for the inlet flow variables are the actually measured values. The complete set of measured inlet flow variables is, however, hardly ever available. In the absence of such detailed experimental information, uniform profiles are commonly specified for the axial velocity and temperature profiles of the continuous phase flow at the inlet plane. The turbulent kinetic energy is usually assumed to be a percentage, between 3 and 20%, of the inlet flow mean kinetic energy. The kinetic energy dissipation rate at the inlet is then obtained as

$$\varepsilon = (C_{\mu}^{3/4} k^{3/2}) / l_d \qquad (5.1)$$

where l_d, the dissipation length scale, is specified as a fraction of the characteristic length scale at the inlet.

For the particle trajectory and temperature history calculations, the initial velocity and temperature slip values relevant to the particular flow problems are employed in setting the required inlet conditions.

Exit Plane:

At the exit plane, the usual boundary condition imposed for any flow variable, ϕ , is $\partial\phi / \partial n = 0$, where n is the normal to the exit plane. This condition is generally valid if the extent of the computational domain in the primary flow direction is sufficient to ensure fully-developed flow conditions for internal flows or self-similarity for jet flows at the exit plane. Particle trajectory and temperature history computations are discontinued for a computational particle once the particle exits from the computational domain through the exit plane or any other open boundary.

Solid Boundary:

The conventional wall functions approach is used to impose wall boundary conditions on the velocity and temperature as well as the turbulence kinetic energy and its dissipation rate. The presence of particles in a fluid flow has been experimentally observed to influence the boundary layer [Kramer and Depew, 1972] and, as a consequence, the nature of the wall function which is normally used to connect the actual value of a given variable at the wall to the value at the wall-adjacent grid node. During their trajectories, particles that reach the wall either adhere to it as observed in particle erosion problems [Dosanjh and Humphrey, 1984], or collide with the wall and get "reflected" back into the flow domain, usually with an accompanying loss of energy and momentum to the wall. In addition, the high level of shear in the wall vicinity coupled with a particle velocity slip introduces an additional transverse force on the particle which further modifies its subsequent trajectory and behavior in the near-wall region. These effects have not been included in the present study, in which perfectly reflecting boundary conditions have been adopted for the particle-wall interaction, but will be the subject of a future study.

Other generic boundary condition types include the symmetry axis, for which $\partial\phi / \partial n = 0$, where in this case, n is the normal to the symmetry axis, and the open boundary condition which has been used by Leschziner and Rodi [1984], Dosanjh and Humphrey [1984], Amano and Brandt [1984] and Chen and Adeniji-Fashola [1987] for modeling parabolic flows of free jets and wall jets using elliptic formulations. These are described in greater detail by Adeniji-Fashola et al. [1988].

6. EXAMPLE FLOWS

In order to illustrate the multiple-realization particle trajectory modeling scheme for confined turbulent fluid-particle flows described above, two example flow problems - vertical pipe upflow and horizontal coaxial jet flow in a recirculation chamber with a particle-laden central jet and a clean annular jet are examined. 1500 computational particles were found to be adequate in each example for obtaining statistically stationary solutions. Typically, global under-relaxation values of 0.50 were found adequate to ensure the stability of global iterations of which between five and seven were required to obtain globally converged solutions. The results obtained for the numerical simulation of these flows will now be discussed.

VERTICAL PIPE UPFLOW

The experimental data which served as the basis for this example numerical simulation are those of Tsuji et al. [1984] for the upflow of a particle-laden stream in a straight vertical pipe. The experimental flow within the test section is considered to be fully-developed after going through a riser that is 167.5 diameters long.

A 50 X 23 uniform grid distribution was used to discretize the computational domain which had an axial extent of 60 pipe diameters. Figure 3 shows both the experimental data and the numerical predictions of the radial profile of the slip in the axial velocity between the air and the particulate phase. The mean particle size and loading ratio are 200μm and 1.0 respectively. The air velocity is slightly overpredicted in the 0.2R - 0.8R range where R is the pipe radius. However, the prediction accuracy is considered to be good for such a complex system. The radial profile of the axial velocity of the solid phase is particularly well predicted. The location of the cross-over in sign of the slip between the phases is predicted to be closer to the wall, less than 0.1R from the wall, than the 0.2R from the wall that was experimentally observed.

A similar picture obtained for the higher loading ratio of 2.1 is presented in Figure 4. The level of accuracy of the predictions is similar to that of the 1.0 loading ratio case. However, it is the air velocity profile that is better predicted in this case. The solid phase axial velocity is considerably underpredicted in the inner 60 percent of the wall region.

As pointed out earlier, the particulate phase has the effect of modulating

the level of the turbulence intensity. For smaller particle sizes this results in a decrease in the kinetic energy of turbulence. The experimentally observed and numerically predicted turbulence modulation effect for a loading ratio of 3.2 are illustrated in Figure 5. The solid line in the figure shows the predicted radial profile of the turbulence intensity for the corresponding "clean" flow. The predicted level of turbulence intensity is considerably higher than the level observed from experiment. Also, while a greater modulation effect was observed closer to the wall region, the predictions show a reversal in which the greater level of modulation is located closer to the pipe centerline. The imposed wall boundary conditions and wall functions in the numerical scheme are probably responsible for the suppression of the modulation effect in the near-wall region.

The development in the axial direction of the streamwise velocity of the particulate phase for an inlet velocity slip ratio of 0.10 is shown in the contour plot of Figure 6a and a corresponding surface plot in Figure 6b. The ability of the particle trajectory scheme to effectively handle extreme levels of velocity slip was tested by imposing an axial slip velocity of 0.10 at the pipe inlet plane. The figures indicate that a fully developed state was attained in the 60D extent of the computational domain.

HORIZONTAL COAXIAL JET FLOW IN RECIRCULATION CHAMBER

The experimental data of Leavitt [1980] serve as the basis for the numerical simulation of this example. The actual geometry studied is illustrated in the schematic of Figure 7. The primary jet air velocity at inlet is 33 m/s while the corresponding secondary jet air velocity is 42 m/s. Coal particles of a mass mean diameter of 43μm were used to uniformly seed the primary jet and the particle loading ratio is 1.50. The estimated turbulence intensity levels at the inlet are 15 and 18% for the primary and secondary jets respectively. The primary and secondary jet diameters at inlet are 0.0255m and 0.127m respectively while the chamber diameter is 0.206m. The axial extent of the recirculation chamber is 0.926m (36.3 primary jet diameters or 4.5 chamber diameters).

A 41 X 41 non-uniform staggered grid distribution, shown in Figure 8, is used for the numerical study and the computational domain extended to 20D where D is the chamber diameter. The numerical prediction of the evolution of the axial velocity is shown in Figure 9. The corner recirculation zone is seen to extend to about 1.79D. No particles are predicted as reaching this recirculation zone and this is believed to be due to the high chamber-to-primary jet diameter ratio of 8.08 and the positive slope of the shear in the mixing layer between the primary and the secondary jets which will result in a slip-shear transverse force directed towards the centerline. Another interesting observation is that the particle axial velocity starts lo lead that of the fluid from

about the 0.80D axial location and this continues to about the 7.43D axial location downstream of which all axial velocity slip disappears. Particles are seen to have dispersed to the outer extremities of the recirculation chamber by the time the 12.0D axial location is reached. However, it should be remembered that this is only a hypothetical situation since the actual experimental investigation was limited to an axial extent of only 4.5D.

Figure 10 shows the axial evolution of the turbulence intensity. It is observed that up to about the 3.0D axial location, the turbulence intensity in the presence of particles (shown dotted) falls below that of the clean flow in the primary jet portion of the flow but is actually higher for the rest of the chamber in the radial direction. However, beyond the 3.0D axial location, the clean flow turbulence intensity uniformly lags the two-phase intensity at all radial locations for any given axial location. The kinetic energy of turbulence is essentially fully developed at the 5.15D axial location and only a radially uniform decrease in magnitude is observed for the rest of the flow in the axial direction. This is in contrast to the radial profile of the axial velocity which does not become fully developed for both phases until the 12.0 to 15.0 diameter range is reached.

The contour and surface plots of the particle axial velocity are shown in Figures 11a and 11b. These have been normalized with respect to the secondary jet gas velocity at inlet. Since, in contrast to the two-fluid scheme, non-zero values of the particle velocity are not returned for computational cells not visited by any particle during the trajectory calculations, the zero-velocity surface in the plots of Figure 11b also indicate the particle-deficient regions.

The comparison of the limited experimental data available from Leavitt [1980] is currently being undertaken.

7. CONCLUDING REMARKS AND RECOMMENDATIONS FOR FUTURE WORK

The numerical modeling of confined turbulent fluid-particle flows using the multiple-realization particle trajectory scheme has been presented. The performance of the numerical modeling scheme has been tested using data for the upward flow of a fluid-particle stream in a straight vertical pipe and for the horizontal coaxial jet flow in a large recirculation chamber for which the central jet is particle-laden.

The multiple-realization particle trajectory turbulent flow modeling scheme ...

is believed to be a more elegant and accurate approach to the extension of single-particle hydrodynamics to dilute multi-particle systems;

is better able to incorporate additional force terms such as lift, virtual mass and Bassett history terms in the particle equation of motion as appropriate;

needs further investigation in order to improve its computational efficiency and so reduce its huge CPU time requirements;

needs to have the particle-turbulence and particle-wall interactions further investigated to improve prediction accuracy.

ACKNOWLEDGEMENTS

Financial support by the National Research Council and NASA - Marshall Space Flight Center under the NRC Research Associateship Program is gratefully acknowledged.

REFERENCES

Adeniji-Fashola, A. A. and Chen, C. P., "Comprehensive Modeling of Turbulent Particulate Flows Using Eulerian and Lagrangian Schemes", AIAA Paper 87-1347, 1987.

Adeniji-Fashola, A. A., Chen, C. P. and Schafer, C. F., "Numerical Predictions of Two-Phase Gas-Particle Flows Using Eulerian and Lagrangian Schemes", NASA Technical Paper, in preparation, 1988.

Al-Taweel, A. M. and Landau, J., "Turbulence Modulation in Two-Phase Jets", Int. J. Multiphase Flows, 3, p. 341, 1977.

Amano, R. S. and Brandt, H., "Numerical Study of Turbulent Axisymmetric Jets Impinging on a Flat Plate and Flowing Into an Axisymmetric Cavity," J. Fluids Engrg., 106, p. 410, 1984.

Amsden, A. A., Ramshaw, J. D., O'Rourke, P. J. and Dukowicz, J. K. "KIVA: A Computer Program for Two- and Three-Dimensional Fluid Flows With Chemical Reactions and Fuel Sprays", Los Alamos National Laboratory Report LA-10245-MS, 1985.

Basset, A. B., Treatise on Hydrodynamics, Vol. 2, Ch. 22, p. 285, Deighton Bell, London, 1888.

Boussinesq, J., Theory Analytique de la Chaleur, Vol. 2, p. 224, L'Ecole Polytechnique, Paris, 1903.

Chen, C. P. and Wood, P. E., "A Turbulence Closure Model for Dilute Gas Particle Flows", Can. J. Ch. E. 63, p. 349, 1985.

Chen, C. P. and Adeniji-Fashola, A. A., "Heat Transfer in Turbulent Fluid-Solids Flows", 24th AIChE/ASME National Heat Transfer Conference, Pittsburgh, Aug. 9-12, 1987.

Cloutman, L. D., Dukowicz, J. K., Ramshaw, J. D. and Amsden, A. A. "CONCHAS-SPRAY: A Computer Code for Reactive Flows with Fuel Sprays", Los Alamos National Laboratory Report LA-9294-MS, 1982.

Corrsin, S. and Lumley, J., "On the Equation of Motion for a Particle in Turbulent Fluid", App. Sci. Res. A, 6, p. 114, 1956.

Crowe, C. T., Sharma, M. P. and Stock, D. E., "The Particle-Source-In Cell (PSI-Cell) Model for Gas-Droplet Flows", J. Fluid Engrg. 99, p.325, 1977.

Depew, C. A. and Kramer, T. J., "Heat Transfer to Flowing Gas-Solid Mixtures", Adv. in Ht. Trans. 9, p. 113, 1973.

Dosanjh, S. and Humphrey, J. A. C., "The Influence of Turbulence on Erosion by a Particle-Laden Fluid Jet", LBL - 17247, Lawrence Berkeley Laboratory, U. Cal., 1984.

Dukowicz, J. K., "A Particle-Fluid Numerical Model for Liquid Sprays", J. Comp. Phys. 35, p. 229, 1980.

Durst, F., Milojevic, D. and Schonung, B., "Eulerian and Lagrangian Predictions of Particulate Two-Phase Flows: A Numerical Study" Appl. Math. Model., 8, p. 101, 1984.

Gosman, A. D. and Ioannides, E., "Aspects of Computer Simulation of Liquid Fueled Combustors", AIAA Paper 81-0323, 1981.

Harlow, F. H., "The Particle-in-Cell Computing Method in Fluid Dynamics", Methods Comput. Phys., 3, p. 319, 1964.

Hjelmfelt, Jr., A. T. and Mockros, L. F., "Motion of Discrete Particles in a Turbulent Fluid", Appl. Sci. Res., 16, p. 149, 1966.

Hockney, R. W. and Eastwood, J. W., Computer Simulation Using Particles, McGraw-Hill Intl. Book Co., 1981.

Leavitt, D. R. "Effects of Coal Dust and Secondary Swirl on Gas and Particle Mixing Rates in Confined Coaxial Jets", MS Thesis, Bringham Young University, 1980.

Maxey, M. R. and Riley, J. J., "Equation of Motion for a Small, Rigid Sphere in a Non-Uniform Flow", Phys. Fl., 26, p. 883, 1983.

Moderrass, D., Tan, H. and Elghobashi, S., "Two-Component LDA Measurement in a Two-Phase Turbulent Jet", AIAA J. 22, p. 624, 1984.

Oseen, C. W., Hydrodynamik, p. 132, Leipzig, 1927.

Patankar, S. V., Numerical Heat Transfer and Fluid Flow, Hemisphere Pub. Corp./McGraw-Hill Book Co., 1980.

Patankar, S. V. and Spalding, D. B.,"A Calculation Procedure for Heat, Mass and Momentum Transfer in Three-Dimensional Parabolic Flows", Int. J. Ht. Mass Trans., 15, p. 1787, 1972.

Sirignano, W. A., "Fuel Droplet Vaporization and Spray Combustion Theory", Prog. Energy. Comb. Sci., 9, p. 291, 1983.

Smoot, L. D. and Smith, P. J., Coal Combustion and Gasification, Plenum Press, New York, 1985.

Sturgess, G. J., Syed, S. A. and McManus, K. R., "Importance of Inlet Boundary Conditions for Numerical Simulation of Combustor Flows", AIAA Paper 83-1263, 1983.

Tchen, C. M., "Mean Value and Correlation Problems Connected With the Motion of Small Particles Suspended in a Turbulent Fluid", Ph.D. Thesis, Delft, 1947.

Tsuji,Y., Morikawa, Y. and Shiomi, H., "LDV Measurements of an Air-Solid Two-Phase Flow in a Vertical Pipe", J. Fl. Mech., 139, p. 417, 1984.

Westphal, R. V. and Johnston, J. P., "Effect of Initial Conditions on Turbulent Reattachment Downstream of a Backward-Facing Step", AIAA J., 22, p. 1727, 1984.

LIST OF FIGURES

1. Particle Trajectories Through Turbulent Eddies.

2. The PSI-Cell Computational Algorithm.

3. Radial Profiles of Streamwise Velocity in Vertical Pipe Upflow for Solids Loading Ratio of 1.0.

4. Radial Profiles of Streamwise Velocity in Vertical Pipe Upflow for Solids Loading Ratio of 2.1.

5. Modulation Effect of Particles on Turbulence Intensity.

6. Particle Streamwise Velocity Contour and Surface Plots for Vertical Upflow in a Straight Pipe.

7. Schematic of Particle-Laden Coaxial Jet Flow in Large Recirculation Chamber.

8. 41 X 41 Non-Uniform Grid Distribution for Recirculation Chamber Flow Simulation.

9. Development in the Streamwise Direction of the Radial Profile of the Axial Velocity in Recirculation Chamber Flow.

10. Development in the Streamwise Direction of the Radial Profile of the Continuous Phase Turbulence Intensity in Recirculation Chamber Flow.

11. Particle Streamwise Velocity Contour and Surface Plots for Horizontal Flow in Recirculation Chamber.

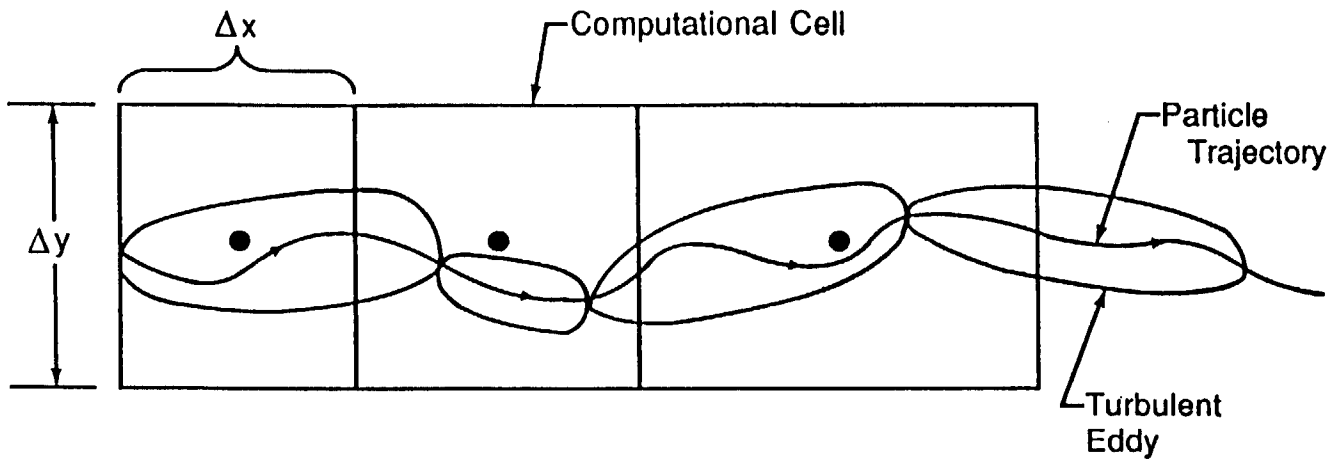

PARTICLE TRAJECTORY THROUGH SUCCESSION OF
TURBULENT EDDIES AND COMPUTATIONAL CELLS

FIGURE 1.

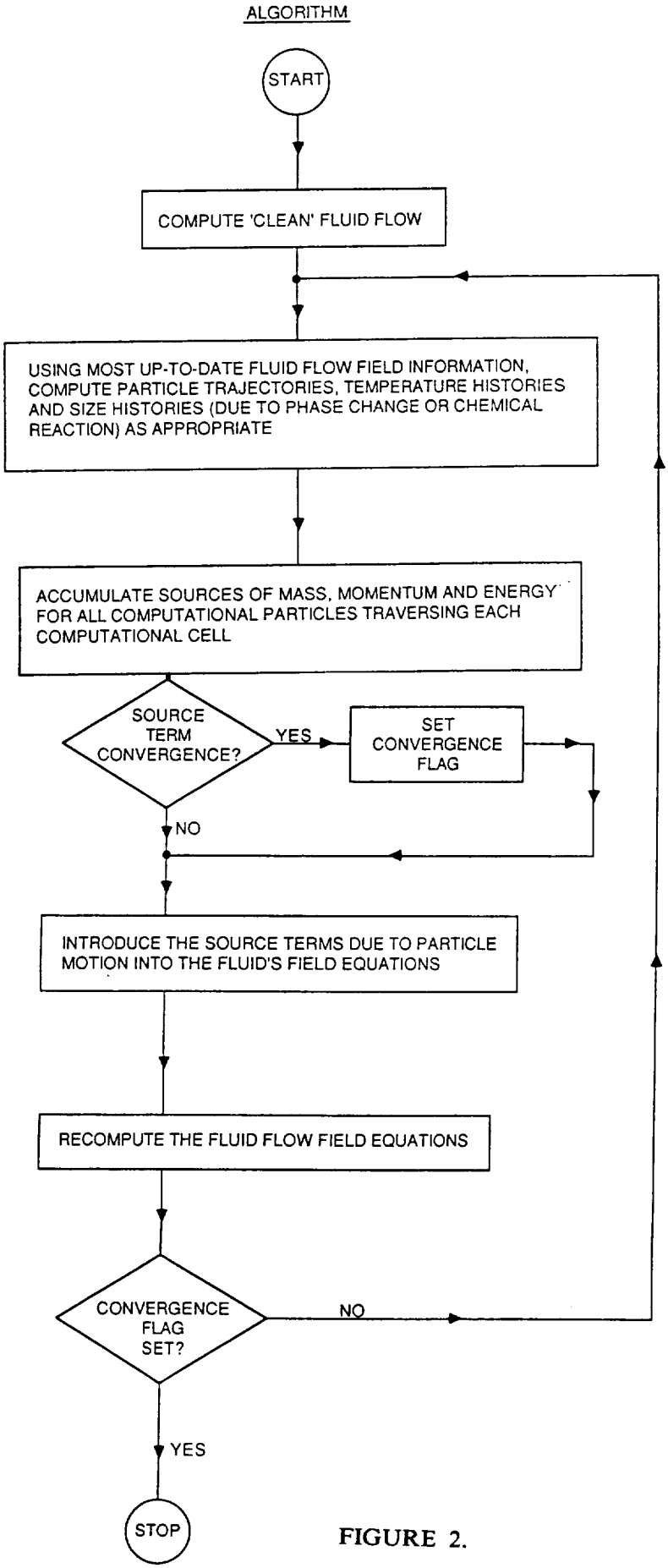
ALGORITHM
START
COMPUTE 'CLEAN' FLUID FLOW
USING MOST UP-TO-DATE FLUID FLOW FIELD INFORMATION, COMPUTE PARTICLE TRAJECTORIES, TEMPERATURE HISTORIES AND SIZE HISTORIES (DUE TO PHASE CHANGE OR CHEMICAL REACTION) AS APPROPRIATE
ACCUMULATE SOURCES OF MASS, MOMENTUM AND ENERGY FOR ALL COMPUTATIONAL PARTICLES TRAVERSING EACH COMPUTATIONAL CELL
SOURCE TERM CONVERGENCE?
YES
SET CONVERGENCE FLAG
NO
INTRODUCE THE SOURCE TERMS DUE TO PARTICLE MOTION INTO THE FLUID'S FIELD EQUATIONS
RECOMPUTE THE FLUID FLOW FIELD EQUATIONS
CONVERGENCE FLAG SET?
NO
YES
STOP

FIGURE 2.

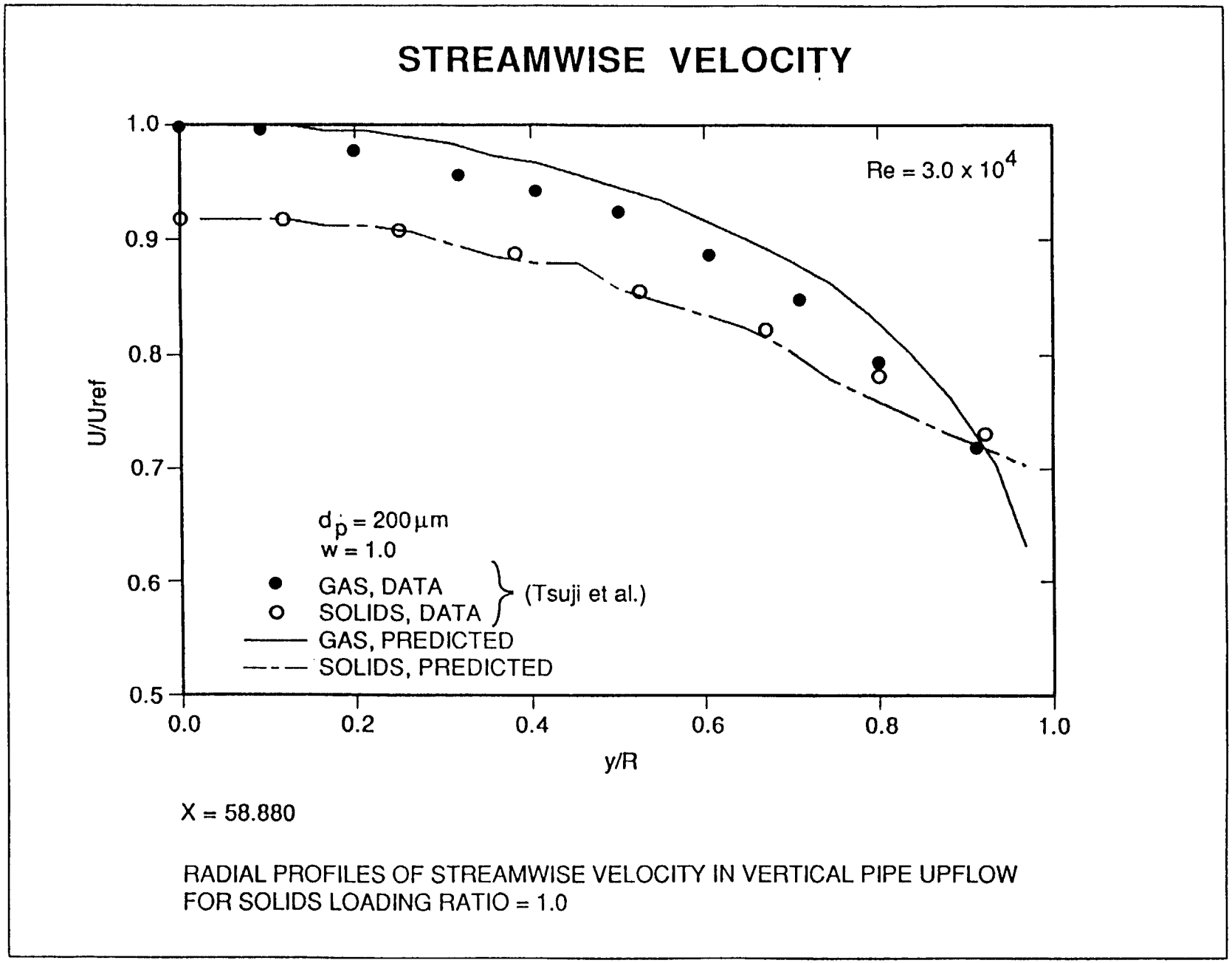
STREAMWISE VELOCITY
Re = 3.0 x 10^4
U/Uref
y/R
1.0
0.9
0.8
0.7
0.6
0.5
0.0
0.2
0.4
0.6
0.8
1.0
d_p = 200 μm
w = 1.0
GAS, DATA
SOLIDS, DATA
(Tsuji et al.)
GAS, PREDICTED
SOLIDS, PREDICTED
X = 58.880
RADIAL PROFILES OF STREAMWISE VELOCITY IN VERTICAL PIPE UPFLOW
FOR SOLIDS LOADING RATIO = 1.0

FIGURE 3.

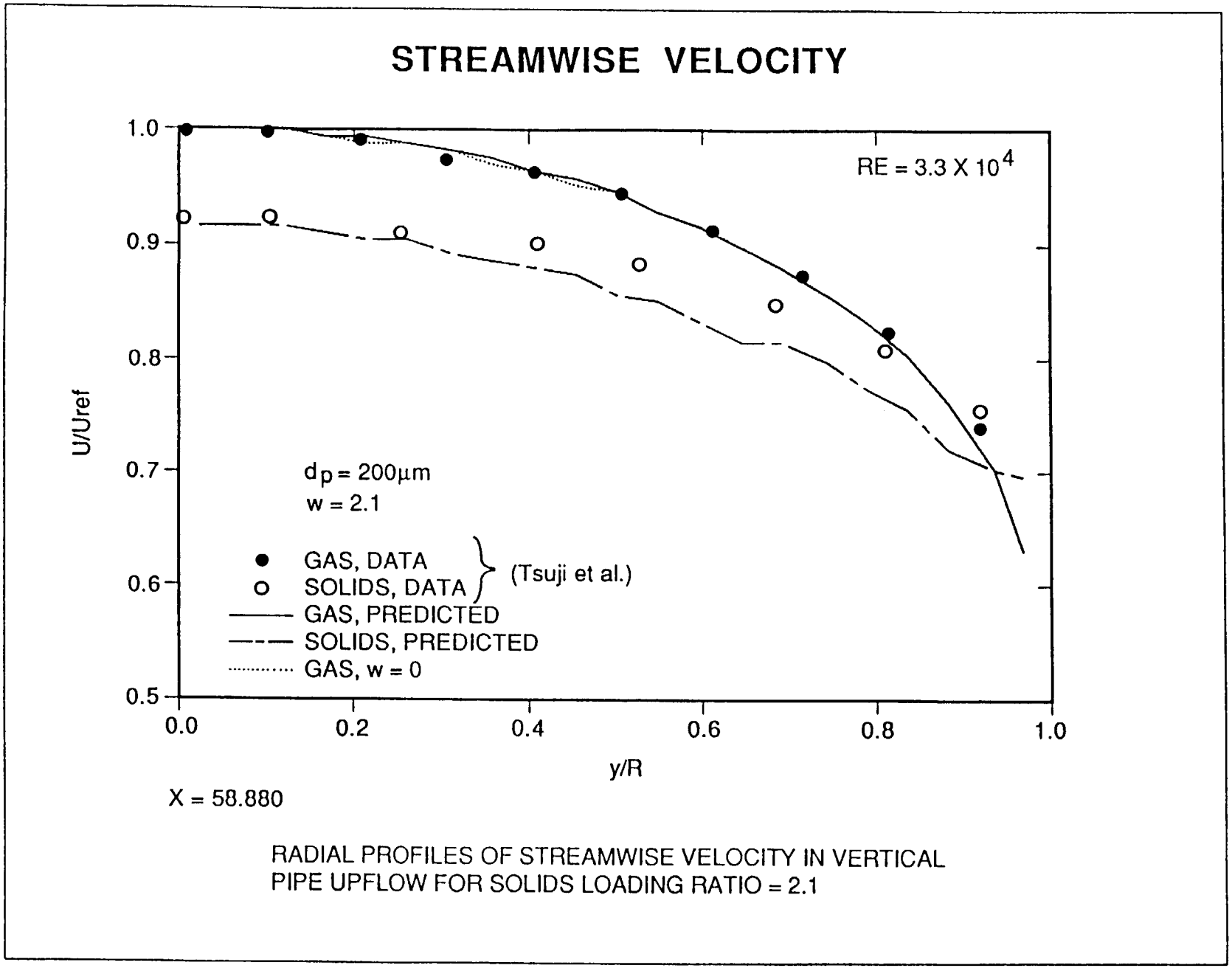

RADIAL PROFILES OF STREAMWISE VELOCITY IN VERTICAL PIPE UPFLOW FOR SOLIDS LOADING RATIO = 2.1

FIGURE 4.

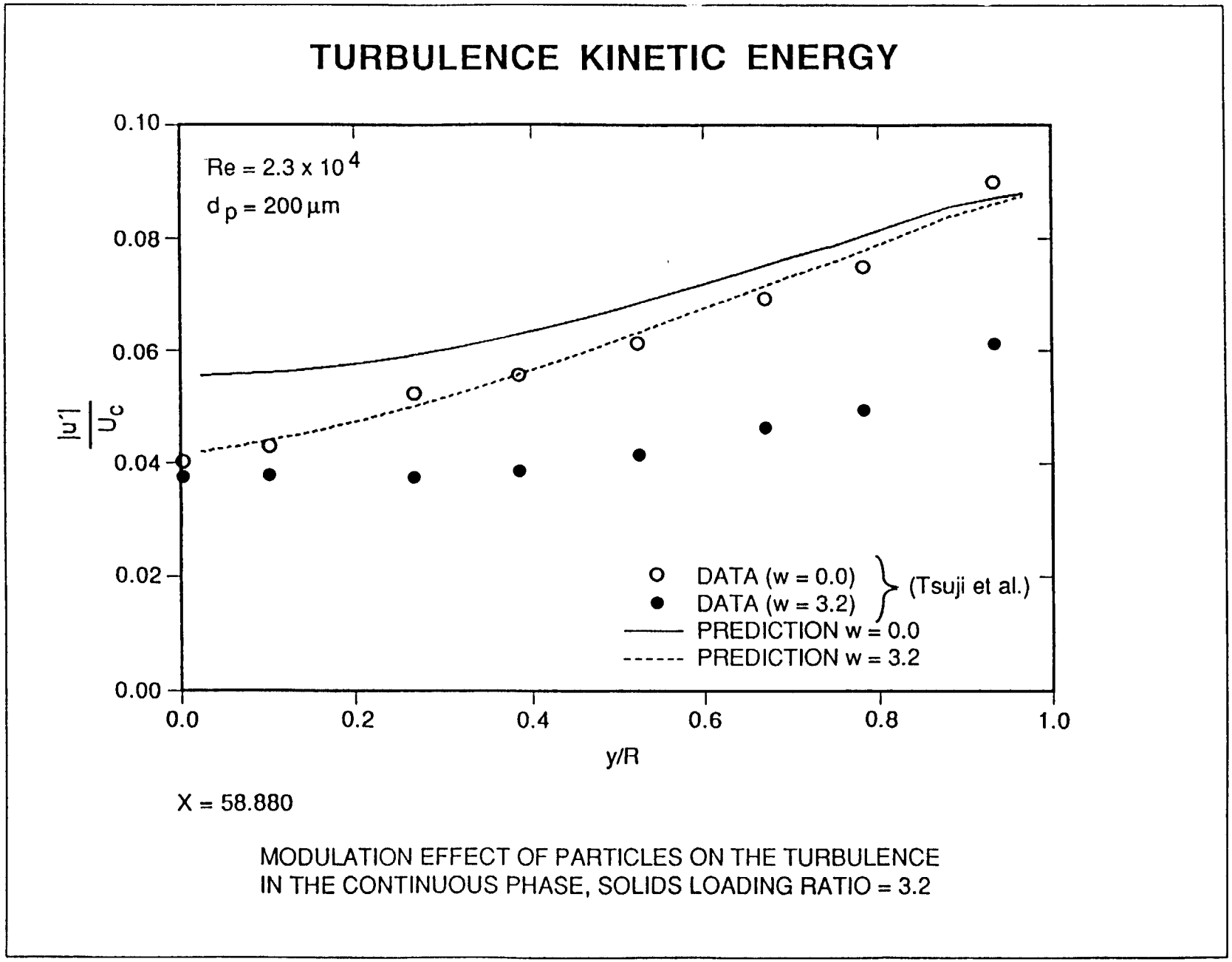
TURBULENCE KINETIC ENERGY
Re = 2.3 x 10^4
d_p = 200 μm
0.10
0.08
0.06
0.04
0.02
0.00
|u'|/U_c
0.0
0.2
0.4
0.6
0.8
1.0
y/R
DATA (w = 0.0)
DATA (w = 3.2)
(Tsuji et al.)
PREDICTION w = 0.0
PREDICTION w = 3.2
X = 58.880
MODULATION EFFECT OF PARTICLES ON THE TURBULENCE
IN THE CONTINUOUS PHASE, SOLIDS LOADING RATIO = 3.2

FIGURE 5.

FIGURE 6.

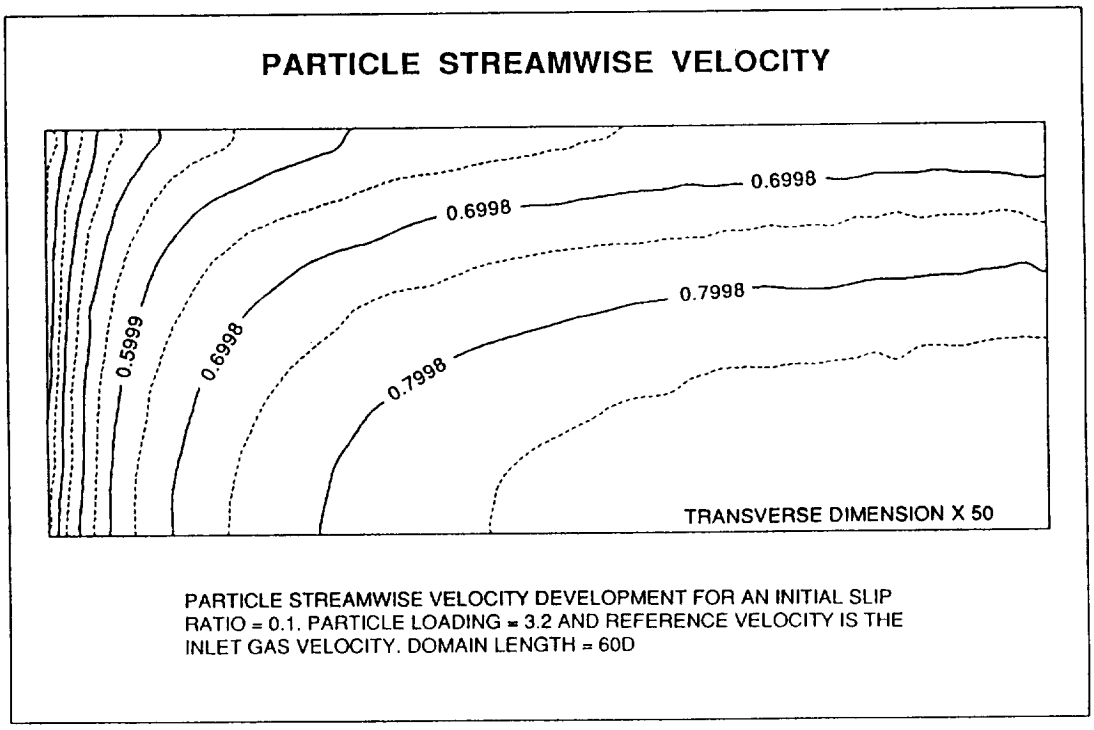

PARTICLE STREAMWISE VELOCITY DEVELOPMENT FOR AN INITIAL SLIP RATIO = 0.1. PARTICLE LOADING = 3.2 AND REFERENCE VELOCITY IS THE INLET GAS VELOCITY. DOMAIN LENGTH = 60D

(a)

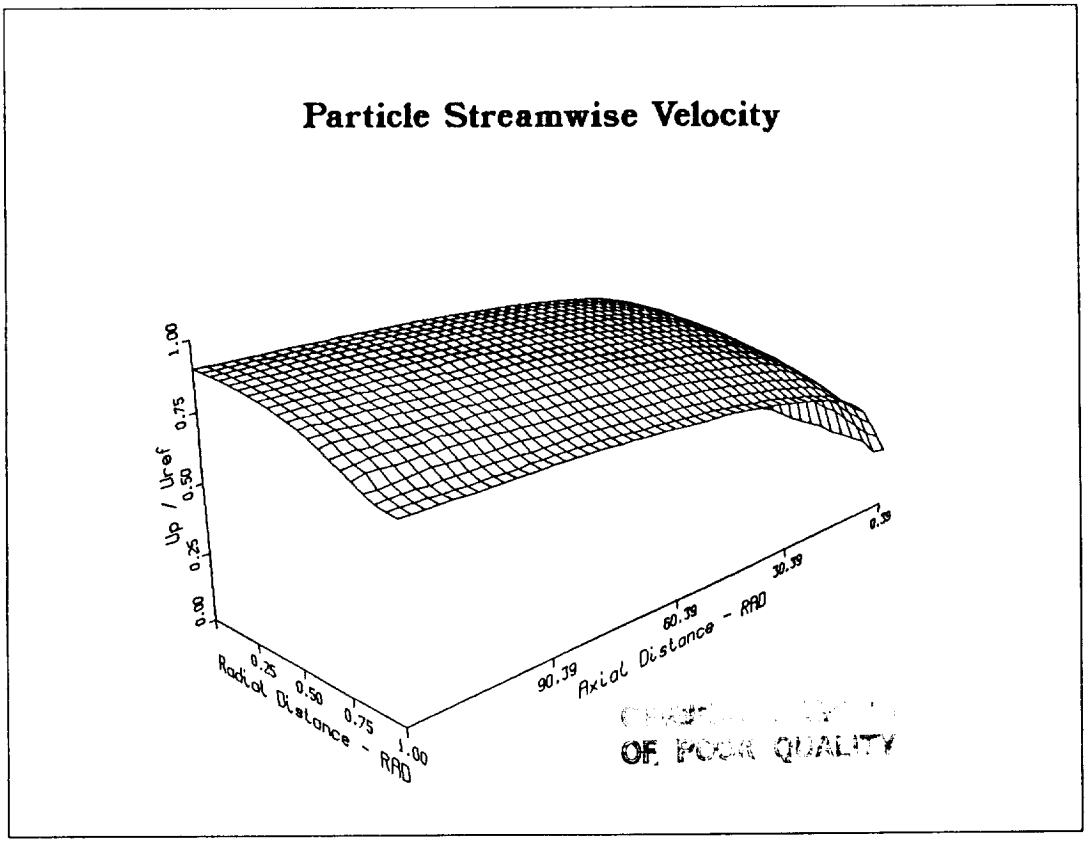

(b)

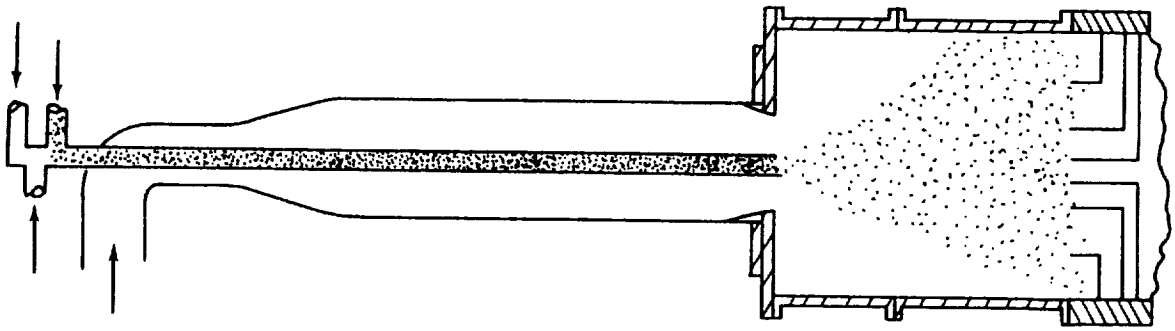

PARTICLE-LADEN FLOW IN LARGE RECIRCULATION CHAMBER

FIGURE 7.

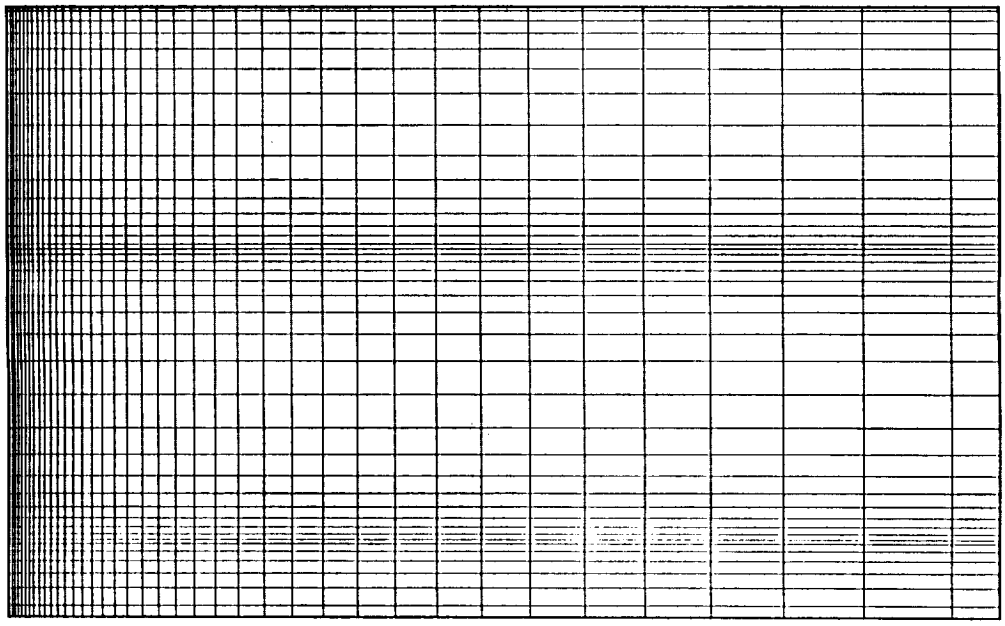

FIGURE 8.

Streamwise Velocity

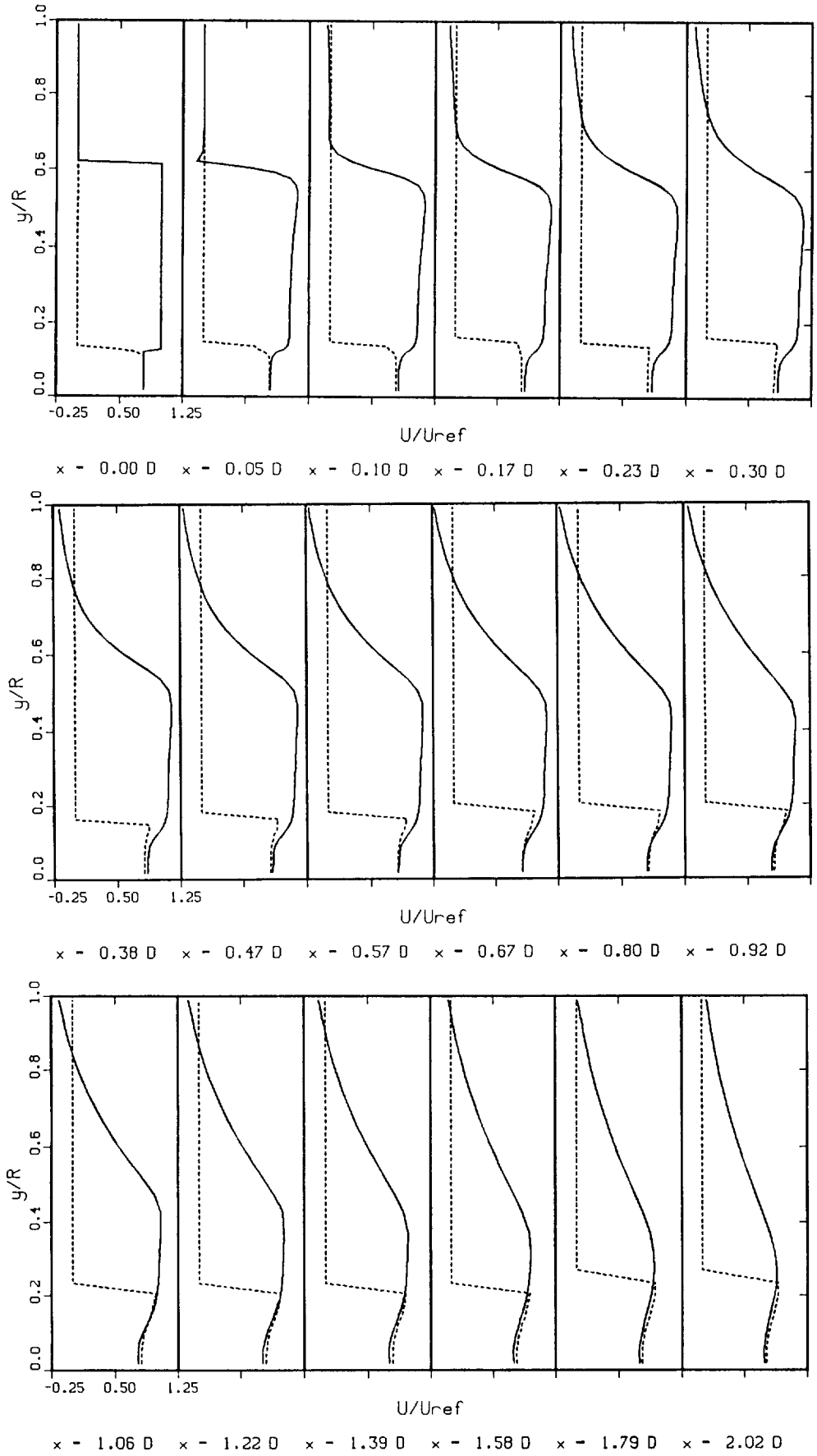

FIGURE 9.

Streamwise Velocity

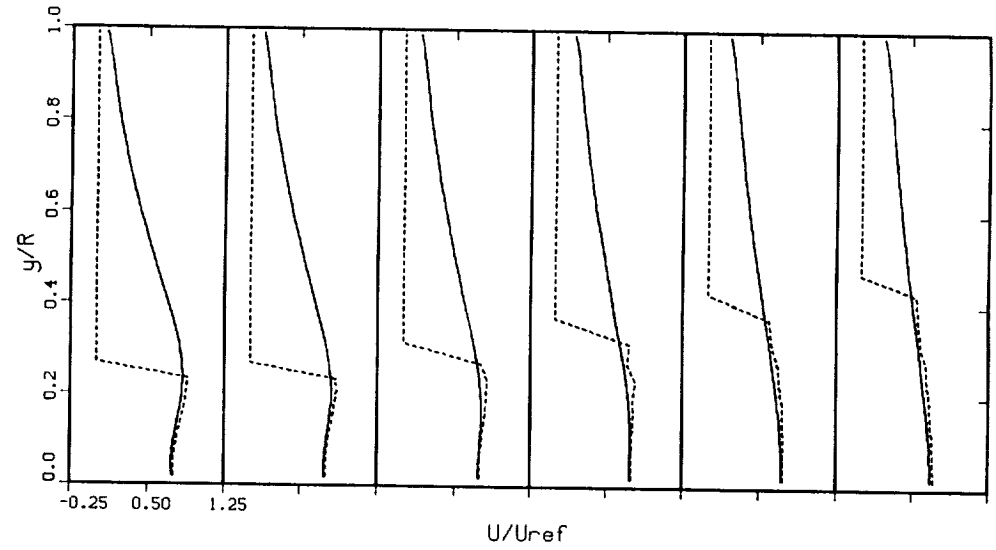

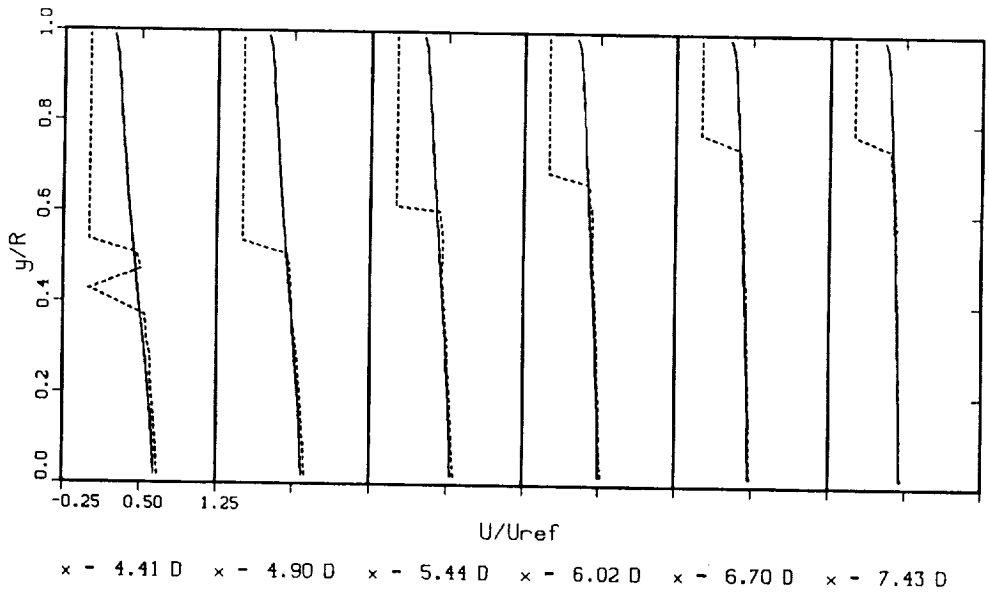

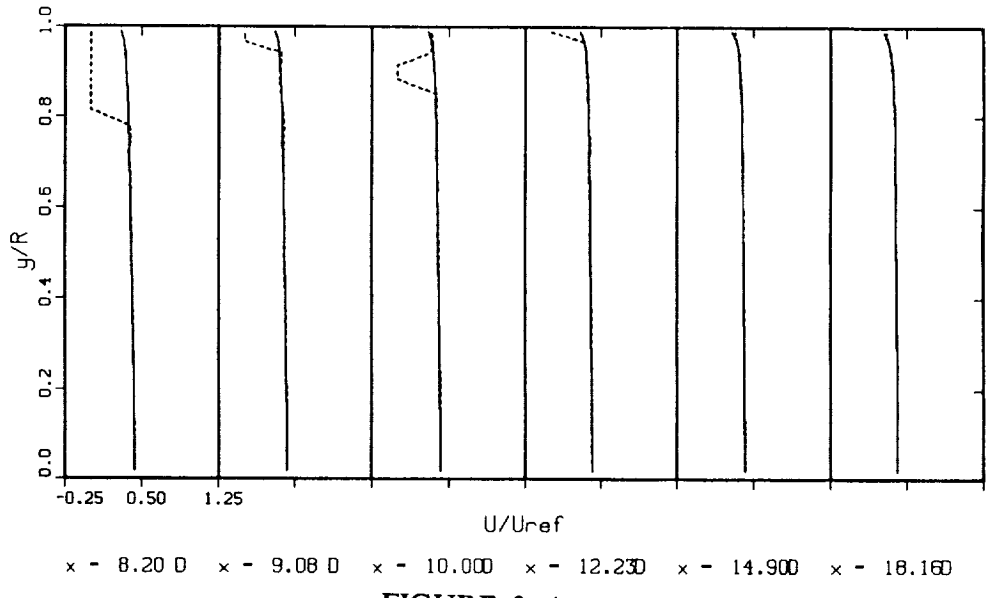

FIGURE 9. (cont.)

Turbulence Kinetic Energy

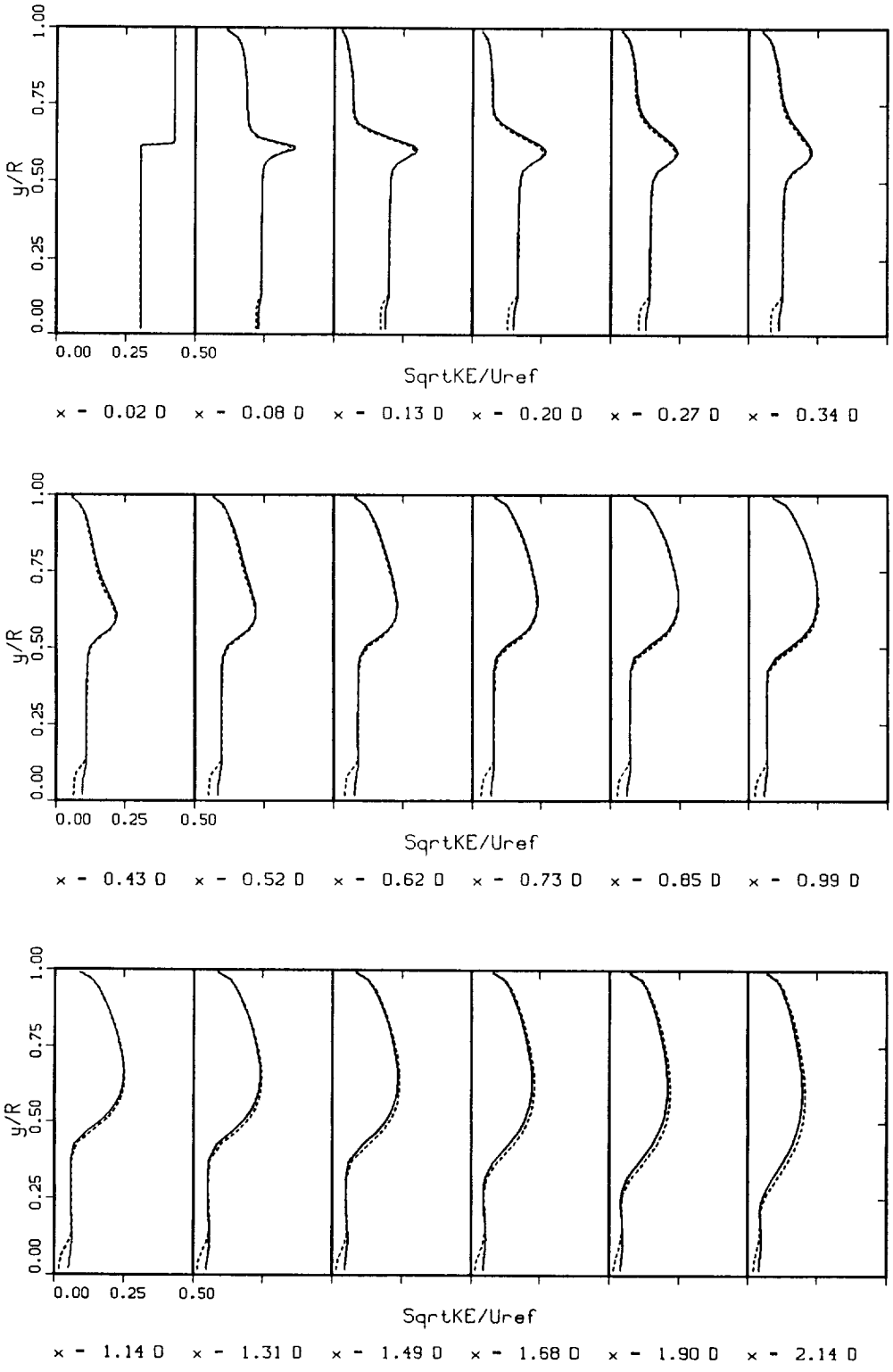

FIGURE 10.

Turbulence Kinetic Energy

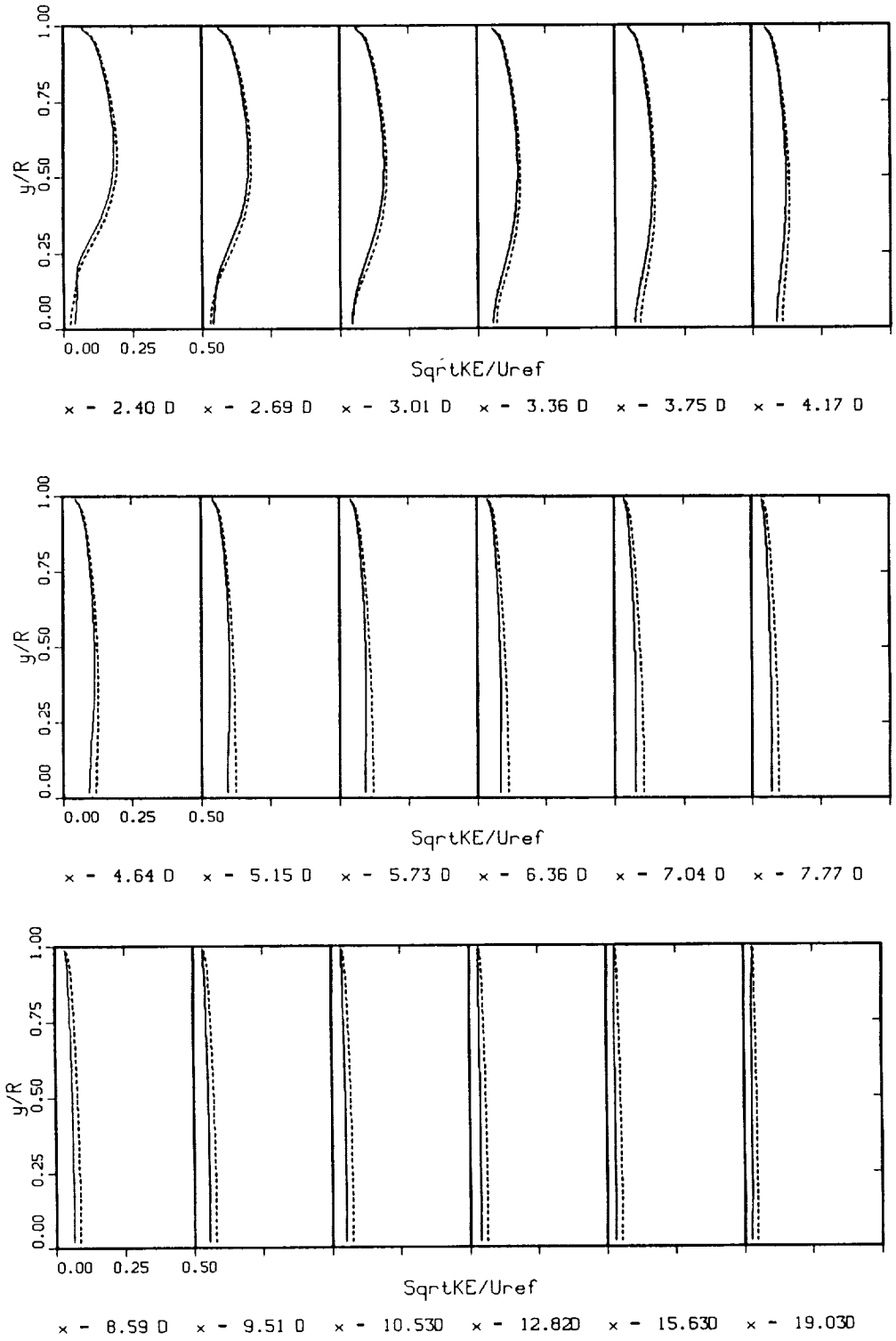

FIGURE 10. (cont.)

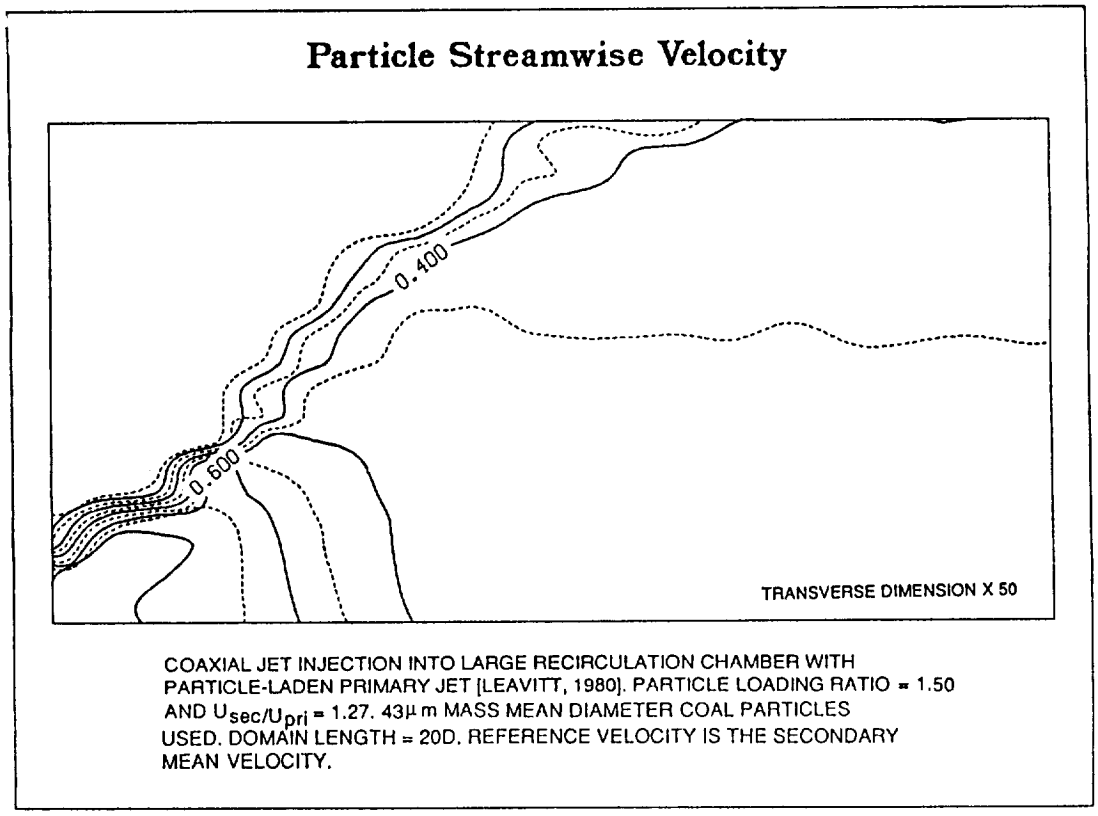
Particle Streamwise Velocity
0.400
0.600
TRANSVERSE DIMENSION X 50
COAXIAL JET INJECTION INTO LARGE RECIRCULATION CHAMBER WITH PARTICLE-LADEN PRIMARY JET [LEAVITT, 1980]. PARTICLE LOADING RATIO = 1.50 AND Usec/Upri = 1.27. 43μm MASS MEAN DIAMETER COAL PARTICLES USED. DOMAIN LENGTH = 20D. REFERENCE VELOCITY IS THE SECONDARY MEAN VELOCITY.

(a)

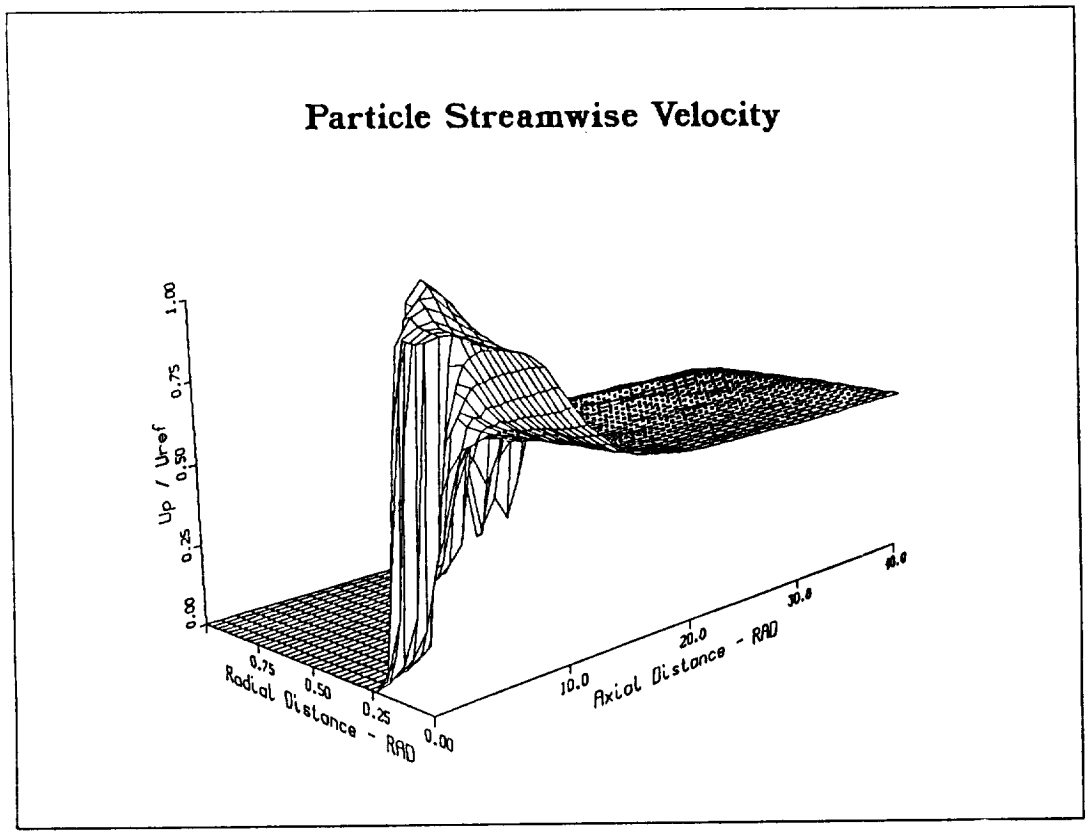
Particle Streamwise Velocity
Up / Uref
0.00
0.25
0.50
0.75
1.00
Radial Distance - RAD
0.00
0.25
0.50
0.75
Axial Distance - RAD
10.0
20.0
30.0

(b)

FIGURE 11.